

Connection between in-plane upper critical field H_{c2} and gap symmetry in layered d -wave superconductors revisited

Jing-Rong Wang,^{1,2,*} Guo-Zhu Liu,^{1,†} and Chang-Jin Zhang^{2,3}

¹*Department of Modern Physics, University of Science and Technology of China, Hefei, Anhui 230026, P. R. China*

²*High Magnetic Field Laboratory, Hefei Institutes of Physical Science,
Chinese Academy of Sciences, Hefei 230031, P. R. China*

³*Collaborative Innovation Center of Advanced Microstructures,
Nanjing University, Nanjing 210093, P. R. China*

Angle-resolved upper critical field H_{c2} provides an efficient tool to probe the gap symmetry of unconventional superconductors. We revisit the behavior of in-plane H_{c2} in d -wave superconductors by considering both the orbital effect and Pauli paramagnetic effect. After carrying out systematic analysis, we show that the maxima of H_{c2} could be along either nodal or antinodal directions of a d -wave superconducting gap, depending on the specific values of a number of tuning parameters. This behavior is in contrast to the common belief that the maxima of in-plane H_{c2} are along the direction where the superconducting gap takes its maximal value. Therefore, identifying the precise d -wave gap symmetry through fitting experiments results of angle-resolved H_{c2} with model calculations at a fixed temperature, as widely used in previous studies, is difficult and practically unreliable. However, our extensive analysis of angle-resolved H_{c2} show that there is a critical temperature T^* : in-plane H_{c2} exhibits its maxima along nodal directions at $T < T^*$ and along antinodal directions at $T^* < T < T_c$. The concrete value of T^* may change as other parameters vary, but the existence of $\pi/4$ shift of H_{c2} at T^* appears to be a general feature. Thus a better method to identify the precise d -wave gap symmetry is to measure H_{c2} at a number of different temperatures, and examine whether there is a $\pi/4$ shift in its angular dependence at certain T^* . We further show that Landau level mixing does not change this general feature. However, in the presence of Fulde-Ferrell-Larkin-Ovchinnikov state, the angular dependence of H_{c2} becomes quite complicated, which makes it more difficult to determine the gap symmetry by measuring H_{c2} . Our results indicate that some previous studies on the gap symmetry of CeCu₂Si₂ are unreliable and need to be reexamined, and also provide a candidate solution to an experimental discrepancy in the angle-resolved H_{c2} in CeCoIn₅.

PACS numbers: 74.20.Rp, 74.25.Op, 74.70.Tx

I. INTRODUCTION

Identifying the precise gap symmetry is generically regarded as an important step on the road of searching for the microscopic pairing mechanism of unconventional superconductivity^{1,2}. Different from the isotropic, phonon mediated BCS superconductors, unconventional superconductors are believed to be induced by the strong electron correlations and normally possess an anisotropic non- s -wave superconducting gap. Extensive theoretic studies have found that an anisotropic superconducting gap always leads to an anisotropic, angle dependent in-plane upper critical field H_{c2} ³⁻⁵. Motivated by these studies, the angle-resolved in-plane H_{c2} has recently been widely used to determine the gap symmetry of a number of unconventional superconductors, including cuprate superconductors^{6,7}, heavy fermion superconductors⁸⁻¹⁰, iron based superconductors¹¹, and other types of superconductors such as Sr₂RuO₄¹² and K₂Cr₃As₃¹³.

It is widely accepted that cuprate superconductors have a $d_{x^2-y^2}$ wave gap^{14,15}. However, the precise gap symmetry of many heavy fermion superconductors is still unclear. Among the dozens of known heavy fermion compounds, CeCu₂Si₂ and CeCoIn₅ have attracted special experimental and theoretical interest¹⁶⁻²⁰.

As the first heavy fermion superconductor²¹, CeCu₂Si₂

has been studied for more than three decades, but no consensus has been reached concerning its precise gap symmetry. A number of earlier experiments provides evidence for a $d_{x^2-y^2}$ -wave gap^{22,23}. Subsequent studies of angle-resolved H_{c2} by Vieyra *et al.*¹⁰ found that the in-plane H_{c2} exhibits a fourfold oscillation with its maxima being along the [100] direction. By fitting model computations to their measurements, Vieyra *et al.*¹⁰ proposed that the gap symmetry of CeCu₂Si₂ should be d_{xy} -wave, which is in sharp contrast to most previous works^{22,23}. Recent specific heat measurements suggested that CeCu₂Si₂ may have a nodeless multi-band superconducting gap²⁴, which challenges the widely accepted notion that the gap symmetry of this superconductor is d -wave. Observations made in the vortex state by scanning tunneling microscopy and spectroscopy are consistent with a multi-band gap with nodes²⁵. First-principle calculations speculated that a promising pairing state might be multi-band s_{\pm} -wave with loop shaped nodes²⁶. Moreover, by measuring the change of penetration depth and renormalized superfluid density, and then comparing these findings to previous measurements of specific heat, a nodeless $d + d$ band-mixing state was also proposed as a candidate for the gap symmetry of CeCu₂Si₂²⁷.

CeCoIn₅, discovered in 2001 by Petrovic *et al.*²⁸, is known to have one of the highest critical temperature, roughly $T_c = 2.3$ K, among the whole heavy fermion fam-

ily. Many experimental measurements, including thermal conductivity²⁹, specific heat in rotated magnetic field³⁰, differential conductance³¹, inelastic neutron scattering³², and scanning tunneling microscopy^{33,34}, have discovered considerable evidence for a $d_{x^2-y^2}$ -wave superconducting gap. Angle-resolved in-plane H_{c2} has also been used to probe the gap symmetry of CeCoIn₅. However, there is a longstanding experimental discrepancy in the angular dependence of in-plane H_{c2} : some experiments found that the maxima of H_{c2} are along the [110] direction³⁵, whereas other experiments observed the maxima of H_{c2} along the [100] direction^{9,36,37}. This discrepancy is regarded as an open puzzle in this field^{9,38}, and prevents us from reaching a final consensus on the precise gap symmetry of CeCoIn₅.

An external magnetic field couples to the charge and spin degrees of freedom of electrons via the orbital and Zeeman mechanisms, respectively. The former coupling destroys the long-range phase coherence and leads to the mixed state in type-II superconductors. The latter one, called Pauli paramagnetic effect, is believed to play an important role in heavy fermion compounds such as CeCu₂Si₂ and CeCoIn₅^{9,17,21,39,40}. The behavior of H_{c2} is determined by the interplay of these two effects.

It is well established that the in-plane H_{c2} exhibits a fourfold oscillation in d -wave superconductors⁴⁻¹⁰. In earlier calculations including only the orbital effect^{4,5}, H_{c2} was always found to display its maxima along the antinodal directions where the d -wave gap is maximal. Later studies included the Pauli paramagnetic effect^{9,41}, but still concluded that the maxima of H_{c2} are along the antinodal directions. There appears to be *a priori* hypothesis in the literature that a larger superconducting gap necessarily results in a larger H_{c2} , which means that H_{c2} and d -wave gap should exhibit their maxima (minima) at exactly the same azimuthal angles θ . If this hypothesized correspondence is valid, it would be easy to identify the gap symmetry: the gap is $d_{x^2-y^2}$ -wave when the measured H_{c2} exhibits its maxima along the [100] direction; the gap is d_{xy} -wave when the measured H_{c2} exhibits its maxima along the [110] direction.

We emphasize that the above hypothesized connection between in-plane H_{c2} and d -wave gap, though intuitively reasonable, is actually not always correct. If there is only orbital effect, H_{c2} and d -wave gap do display the same angular dependence. However, this connection can be destroyed by the Pauli paramagnetic effect.

In this paper, motivated by the recent progress and the existing controversy, we will analyze the influence of the interplay of orbital and Pauli paramagnetic effect on the behavior of in-plane H_{c2} in d -wave superconductors. The aim of this paper is to provide a better understanding of the properties of the angle-resolved in-plane H_{c2} in CeCu₂Si₂ and CeCoIn₅. After carrying out systematical calculations, we show that the maxima of angle-dependent $H_{c2}(\theta)$ are not necessarily along the antinodal directions in the presence of Pauli paramagnetic effect. Interestingly, the angular dependence of H_{c2} is deter-

mined by a number of parameters, including temperature T , critical temperature T_c , gyromagnetic ratio g , fermion velocity v_0 , and two parameters that characterize the shape of the corresponding Fermi surface. Any of these six parameters can drive a $\pi/4$ shift in the fourfold oscillation pattern of H_{c2} . Since approximations are inevitable in theoretical calculations, it is technically quite difficult to identify whether the precise gap symmetry is $d_{x^2-y^2}$ wave or d_{xy} wave by fitting experimental results with model calculations at a fixed temperature. Among the six tuning parameters, the temperature T plays a particular role. If one varies T but fixes all the rest parameters, H_{c2} exhibits its maxima along the nodal directions at $T < T^*$ and antinodal directions at $T > T^*$ due to a sufficiently strong Pauli paramagnetic effect, where T^* is certain critical temperature. The concrete magnitude of T^* may change as other parameters vary, but the existence of a $\pi/4$ shift in the four-fold oscillation of H_{c2} at T^* appears to be general feature. This feature provides a better method to determine the precise gap symmetry by measuring the in-plane H_{c2} at a large number of temperatures and see whether there is a $\pi/4$ shift in its angular dependence.

On the basis of our theoretical results, we find that some previous conclusions about the precise gap symmetry of CeCu₂Si₂ are actually unreliable, and need to be further studied. Moreover, our finding provides a possible solution for an experimental discrepancy in the measured angular dependence of in-plane H_{c2} in CeCoIn₅.

To examine the validity of our conclusion, we will also study the impacts of Landau level mixing and Fulde-Ferrell-Larkin-Ovchinnikov (FFLO) state^{42,43}, which may be important in some heavy fermion compounds. We find that Landau level mixing does not change the general feature that the maxima of H_{c2} shifts by $\pi/4$ at critical temperature T^* . In the presence of FFLO state, however, the maximum of H_{c2} may be along the nodal or antinodal directions, depending sensitively on the temperature of the system. This makes it more difficult to identify the precise gap symmetry by measuring the angular dependence of H_{c2} .

The rest of paper is organized as follows. In Sec. II, we derive the equation of in-plane H_{c2} for $d_{x^2-y^2}$ superconductor with a rippled cylindrical Fermi surface. In Sec. III, we show the influence of different parameters on H_{c2} by numerical calculations. In Sec. IV, the influences of Landau level mixing and FFLO state on H_{c2} are given. In Sec. V, we then compare our results with experimental studies about angle-resolved H_{c2} . In Sec. VI, we summarize our main results.

II. DERIVATION OF THE EQUATION OF H_{c2}

Many heavy fermion compounds have a layered structure, but the inter-layer coupling cannot be entirely ignored^{18,19,44}. To embody this feature, it is convenient to assume a rippled cylindrical Fermi surface, which is

schematically shown in Fig. 1. Now the fermion momentum \mathbf{k} should have three components: $k_{x,y}$ denote the x, y -components in the basic superconducting plane, and k_z denotes the z -component along c -axis. We use t_c to represent the inter-layer hopping parameter and c the unit size along z -direction. The dispersion relation of fermions is given by^{45,46},

$$\varepsilon(\mathbf{k}) = \frac{1}{2m}(k_x^2 + k_y^2) - 2t_c \cos(\chi) \quad (1)$$

with $\chi = k_z c$. Superconductivity is entirely suppressed once the in-plane field H reaches H_{c2} , which can be obtained by solving a linearized gap equation. Near the second-order transition, the gap function has the form

$$\Delta(\mathbf{R}, \mathbf{k}) = \Delta_\alpha(\mathbf{R})\gamma_\alpha(\hat{\mathbf{k}}), \quad (2)$$

where $\gamma_\alpha(\hat{\mathbf{k}})$ reflects the symmetry of the gap function and α may correspond to $s, d_{x^2-y^2}, d_{xy}$, and so on. Employing the general methods presented in Refs.⁴⁷⁻⁵⁴, we find the following equation

$$\begin{aligned} -\ln\left(\frac{T}{T_c}\right)\Delta_\alpha(\mathbf{R}) &= \int_0^{+\infty} d\eta \frac{\pi T}{\sinh(\pi T \eta)} \int_{-\pi}^{\pi} \frac{d\chi}{2\pi} \int_0^{2\pi} \frac{d\varphi}{2\pi} \\ &\times \gamma_\alpha^2(\hat{\mathbf{k}}) \left\{ 1 - \cos \left[\eta \left(h' + \frac{1}{2} \mathbf{v}_F(\hat{\mathbf{k}}) \cdot \boldsymbol{\Pi}(\mathbf{R}) \right) \right] \right\} \Delta_\alpha(\mathbf{R}). \end{aligned} \quad (3)$$

In the simplest case, we now neglect the influence of Landau level mixing and FFLO state. Their influence will be considered separately in Sec.IV. Assuming that $\Delta_\alpha(\mathbf{R}) = \Delta_0(\mathbf{R})$, we have

$$\Delta_0(\mathbf{R}) = \left(\frac{2eH}{\pi} \right)^{\frac{1}{4}} e^{-eH(x \sin \theta - y \cos \theta)^2}, \quad (4)$$

where $\Delta_0(\mathbf{R})$ is the lowest Landau level, and θ is the angle between the direction of in-plane magnetic field and the x -axis, corresponding to the $[100]$ direction, within the basal plane. The generalized derivative operator is defined as

$$\boldsymbol{\Pi}(\mathbf{R}) = -i\nabla_{\mathbf{R}} + 2e\mathbf{A}(\mathbf{R}), \quad (5)$$

where the vector potential is chosen to be

$$\mathbf{A}(\mathbf{R}) = H(-x \sin \theta + y \cos \theta) \mathbf{e}_z. \quad (6)$$

Now the field \mathbf{H} takes the form

$$\mathbf{H} = \nabla \times \mathbf{A} = H \cos \theta \mathbf{e}_x + H \sin \theta \mathbf{e}_y. \quad (7)$$

For a rippled cylindrical Fermi surface, the vector of Fermi velocity is given by⁴⁶

$$\mathbf{v}_F(\hat{\mathbf{k}}) = v_a \cos \varphi \mathbf{e}_x + v_a \sin \varphi \mathbf{e}_y + v_c \sin \chi \mathbf{e}_z. \quad (8)$$

Here, $v_c = 2t_c c$, and $v_a = v_0 \sqrt{1 + \lambda \cos(\chi)}$, where $v_0 = \frac{k_{F0}}{m}$ with Fermi momentum k_{F0} being related to

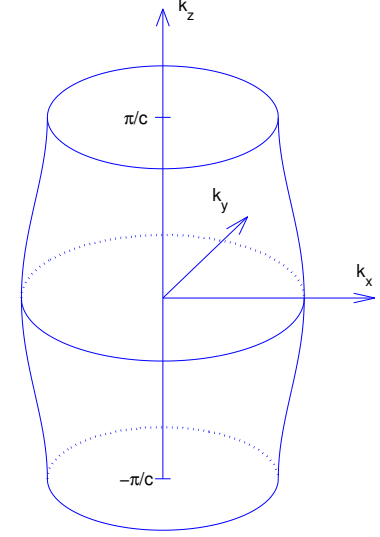


FIG. 1: Schematic diagram for a rippled cylindrical Fermi surface.

Fermi energy ϵ_F by $k_{F0} = \sqrt{2m\epsilon_F}$. The shape of rippled cylindrical Fermi surface is characterized by a velocity ratio $v_c/v_0 = \lambda\gamma$, where $\lambda = 2t_c/\epsilon_F$ and $\gamma = ck_{F0}/2$. As will be shown later, both λ and γ can strongly affect the behavior of H_{c2} . Moreover, we define $h' = -\frac{g\mu_B H}{2}$, where μ_B is Bohr magneton and g gyromagnetic ratio. The orbital effect is encoded in the factor $\mathbf{v}_F(\mathbf{k}) \cdot \boldsymbol{\Pi}(\mathbf{R})$, whereas the Pauli paramagnetic effect is represented by the factor h' . The concrete angular dependence of H_{c2} is determined by the interplay of these two effects.

To facilitate analytical computation, we can choose the direction of field \mathbf{H} as a new z' -axis and define

$$\begin{cases} \mathbf{e}'_x = \mathbf{e}_x \sin \theta - \mathbf{e}_y \cos \theta \\ \mathbf{e}'_y = -\mathbf{e}_z \\ \mathbf{e}'_z = \mathbf{e}_x \cos \theta + \mathbf{e}_y \sin \theta \end{cases}. \quad (9)$$

In the coordinate frame spanned by $(\mathbf{e}'_x, \mathbf{e}'_y, \mathbf{e}'_z)$, we write the velocity vector as

$$\mathbf{v}_F(\hat{\mathbf{k}}) = v_a \sin(\theta - \varphi) \mathbf{e}'_x - v_c \sin \chi \mathbf{e}'_y + v_a \cos(\theta - \varphi) \mathbf{e}'_z,$$

and the generalized derivative operator as

$$\begin{aligned} \boldsymbol{\Pi}(\mathbf{R}) &= \sqrt{eH} [(a_+ + a_-) \mathbf{e}'_x - i(a_+ - a_-) \mathbf{e}'_y \\ &\quad + \sqrt{2}a_0 \mathbf{e}'_z], \end{aligned} \quad (10)$$

where

$$a_{\pm} = \frac{1}{2\sqrt{eH}} [-i \sin \theta \partial_x + i \cos \theta \partial_y \mp \partial_z \pm 2ieH(x \sin \theta - y \cos \theta)], \quad (11)$$

$$a_0 = \frac{1}{\sqrt{2eH}} [-i \partial_x \cos \theta - i \partial_y \sin \theta], \quad (12)$$

which satisfy

$$[a_-, a_+] = 1, [a_{\pm}, a_0] = 0. \quad (13)$$

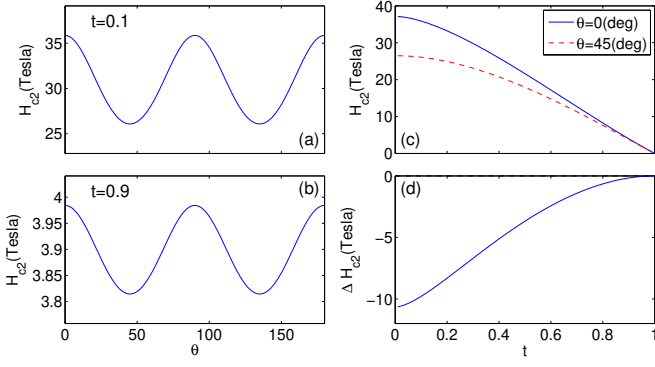


FIG. 2: (a) and (b): Fourfold oscillation of θ -dependent H_{c2} at $t = 0.1$ and $t = 0.9$; (c) and (d): t -dependence of H_{c2} and ΔH_{c2} with $T_c = 1K$, $v_0 = 3000m/s$, $\lambda = 0.5$, and $\gamma = 1$. Only orbital effect is considered.

In Eq. (3), the influence of gap symmetry is reflected in $\gamma_\alpha(\hat{\mathbf{k}})$. For s -wave gap, $\gamma_s(\hat{\mathbf{k}}) = 1$; for $d_{x^2-y^2}$ -wave gap, $\gamma_{d_{x^2-y^2}}(\hat{\mathbf{k}}) = \sqrt{2}\cos(2\varphi)$; for d_{xy} -wave gap, $\gamma_{d_{xy}}(\hat{\mathbf{k}}) = \sqrt{2}\sin(2\varphi)$. Now we take $d_{x^2-y^2}$ -wave gap as an example, so $\gamma_{d_{x^2-y^2}}(\hat{\mathbf{k}}) = \sqrt{2}\cos(2\varphi)$. The results for d_{xy} -wave gap can be obtained analogously, and the main conclusion does not change. Averaging over $\Delta(\mathbf{R})$ on both sides of Eq. (3) and inserting $\gamma_{d_{x^2-y^2}}(\hat{\mathbf{k}})$, we obtain

$$-\ln t = \int_0^{+\infty} \frac{du}{\sinh(u)} \left\{ 1 - \int_{-\pi}^{\pi} \frac{d\chi}{2\pi} \int_0^{2\pi} \frac{d\varphi}{2\pi} \times \cos(hu) [1 + \cos(4\theta) \cos(4\varphi)] \times e^{-\rho u^2 (\lambda^2 \gamma^2 \sin^2 \chi + (1 + \lambda \cos \chi) \sin^2 \varphi)} \right\}, \quad (14)$$

where $t = \frac{T}{T_c}$, $h = \frac{g\mu_B H_{c2}}{2\pi k_B T}$ and $\rho = \frac{v_0^2 e H_{c2}}{8\pi^2 k_B^2 T^2}$. For the detailed derivation of Eq. (14), please see the Appendix.

Although the linearized gap equation (14) is formally general and valid in many superconductors, its solution is determined by a number of physical effects and associated parameters. From Eq. (14), we see $H_{c2}(\theta)$ depends on six physical parameters: critical temperature T_c , temperature ratio $t = T/T_c$, velocity v_0 , gyromagnetic ratio g , $\lambda = 2t_c/\epsilon_F$, and $\gamma = k_F c/2$. Among these parameters, λ and γ are related to the shape of the rippled cylindrical Fermi surface. We notice that the influence of λ and γ were not carefully investigated in previous works on H_{c2} .

In previous studies on this problem⁸⁻¹⁰, a rippled cylindrical Fermi surface is often assumed, but there is not any tuning parameter in the equation of H_{c2} that can characterize how rippled is the Fermi surface. In our equation of H_{c2} , given by Eq. (14), we have introduced two tuning parameters λ and γ to characterize the concrete shape of the rippled Fermi surface. In the next section, we will show that whether the maxima of H_{c2} is along the nodal or antinodal direction depends on the specific values of these two parameters. Apparently, the

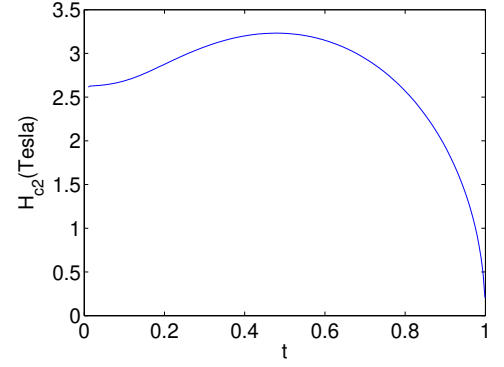


FIG. 3: t -dependence of H_{c2} caused solely by Pauli paramagnetic effect. $T_c = 1K$, $\lambda = 0.5$, $\gamma = 1$, and $g = 1$.

shape of the Fermi surface can significantly influence the angular dependence of H_{c2} , which is not properly considered in previous works. In addition, in previous studies of H_{c2} ⁸⁻¹⁰, the precise d -wave gap symmetry is identified by comparing theoretical calculations to experimental results of H_{c2} at a fixed temperature. In the next section, we will prove that varying the temperature leads to a $\pi/4$ shift of angle-resolved H_{c2} . This striking temperature dependence of angle-resolved H_{c2} has not been realized previously. According to this property, measuring H_{c2} and then fitting experiments with model calculations at a given temperature may yield incorrect conclusion about the precise gap symmetry.

III. ANGULAR DEPENDENCE OF H_{c2} AND ITS CONNECTION WITH GAP SYMMETRY

In this section, we present the numerical results for in-plane H_{c2} by solving Eq. (14) numerically and discuss the influence of various parameters on the angular dependence of H_{c2} .

The detailed behavior of H_{c2} can be clearly seen from its angular dependence. In addition, it is equally important to analyze the difference of H_{c2} between its values obtained at $\theta = 45^\circ$ and $\theta = 0^\circ$, i.e., $\Delta H_{c2} = H_{c2}(\theta = 45^\circ) - H_{c2}(\theta = 0^\circ)$ since the maxima and minima of H_{c2} always appear at these two angles. H_{c2} exhibits its maxima at $\theta = 45^\circ$ if $\Delta H_{c2} > 0$ and at $\theta = 0^\circ$ if $\Delta H_{c2} < 0$.

First, we consider only the orbital effect by setting $g = 0$. In this case, the factor $\cos(hu)$ appearing in Eq. (14) is equal to unity, $\cos(hu) = 1$. We assume that $T_c = 1K$, $v_0 = 3000m/s$, $\lambda = 0.5$, and $\gamma = 1$, which are suitable parameters for heavy fermion compounds.

After carrying out numerical calculations, we plot the angular dependence of $H_{c2}(\theta)$ in Fig. 2 at two representative temperatures $t = 0.1$ and $t = 0.9$. Figure 2 clearly shows that $H_{c2}(\theta)$ exhibits a fourfold oscillation pattern. The maxima of H_{c2} is always along the antinodal directions for any values of relevant parameters, which means that the angular dependence of orbital effect-induced H_{c2}

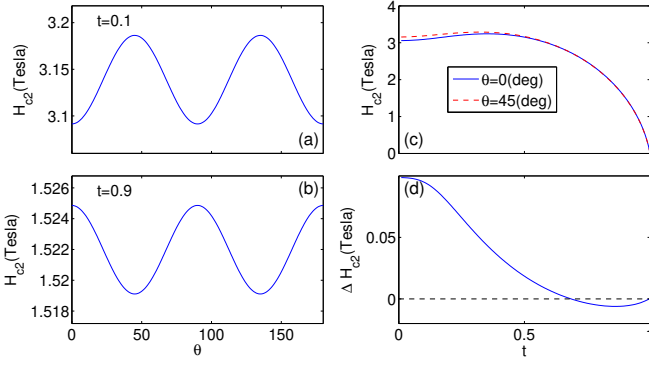


FIG. 4: (a) and (b): Angular dependence of H_{c2} at $t = 0.1$ and $t = 0.9$. $T_c = 1K$, $v_0 = 3000m/s$, $\lambda = 0.5$, $\gamma = 1$, and $g = 1$. (c) and (d): t -dependence of H_{c2} and ΔH_{c2} . Both the orbital and Pauli effects are considered.

is exactly the same as that of the gap. This is consistent with previous results of Refs.^{4,5}. Moreover, the positions of peaks are t -independent. H_{c2} is a monotonic decreasing function of t , since the gap is suppressed as t grows. Moreover, ΔH_{c2} is negative for all values of t .

We next consider the influence of pure Pauli paramagnetic effect on H_{c2} by setting $v_0 = 0$, which leads to

$$-\ln(t) = \int_0^{+\infty} du \frac{1 - \cos(hu)}{\sinh(u)}. \quad (15)$$

This equation is completely independent of θ . The t -dependence of H_{c2} is shown in Fig. 3. H_{c2} is not a monotonic function: it first rises with growing t , but decreases when t is sufficiently large.

Finally we come to the interplay of orbital and Pauli paramagnetic effects, which are both important in some heavy fermion compounds, including $CeCu_2Si_2$ and $CeCoIn_5$. As aforementioned, the angular dependence of H_{c2} is determined by a number of tuning parameters. To make the results as transparent as possible, we vary one single parameter at each time and fix all the rest parameters at certain values.

As shown in Fig. 4, under the chosen parameters, the maxima of H_{c2} locates along the antinodal directions at a relatively higher temperature $t = 0.9$. This behavior is very similar to that in the case of pure orbital effect. However, at a lower temperature $t = 0.1$, the maxima of H_{c2} is along the nodal directions where the $d_{x^2-y^2}$ -wave gap vanishes. Two conclusions can be drawn: (i) H_{c2} does not always exhibit its maxima at the angles where the superconducting gap is maximal; (ii) the fourfold oscillation curves of H_{c2} are shifted by $\pi/4$ as temperature grows across certain critical value T^* .

We see from Fig. 4(c) that H_{c2} first increases with growing t , but decreases rapidly once t exceeds a critical value. Such a non-monotonic t -dependence of H_{c2} is clearly caused by the Pauli paramagnetic effect. Moreover, the difference ΔH_{c2} shown in Fig. 4(d) is positive for small t but becomes negative for larger values of t .

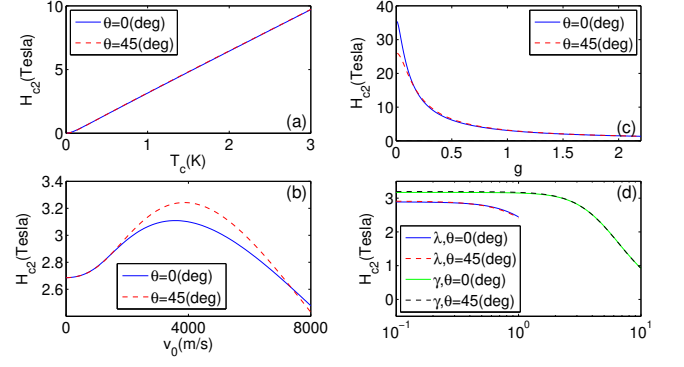


FIG. 5: (a) T_c -dependence of H_{c2} . $t = 0.5$, $v_0 = 3000m/s$, $\lambda = 0.5$, $\gamma = 1$, and $g = 1$. (b) v_0 -dependence of H_{c2} . $t = 0.1$, $T_c = 1K$, $\lambda = 0.5$, $\gamma = 1$, and $g = 1$. (c) g -dependence of ΔH_{c2} . $t = 0.1$, $v_0 = 3000m/s$, $T_c = 1K$, $\lambda = 0.5$, and $\gamma = 1$. (d) Blue solid line and red dashed line: λ -dependence of H_{c2} for $\theta = 0^\circ$ and $\theta = 45^\circ$ respectively. $t = 0.5$, $v_0 = 5000m/s$, $T_c = 1K$, $\gamma = 1$, and $g = 1$; Green solid line and black dashed line: γ -dependence of ΔH_{c2} for $\theta = 0^\circ$ and $\theta = 45^\circ$ respectively. $t = 0.5$, $v_0 = 3000m/s$, $T_c = 1K$, $\lambda = 0.5$, and $g = 1$. Both the orbital and Pauli effects are considered.

T_c : It is well known that T_c of heavy fermion compounds is not high, especially when compared with cuprates and iron pnictides. To make a general analysis, we assume T_c varies between 0K and 3K. All the other parameters are fixed. From Fig. 5(a), we find that H_{c2} increases monotonously as T_c grows. As displayed in Fig. 6(a), if T_c is smaller than some critical value, ΔH_{c2} is negative, which means the maxima of H_{c2} are along the antinodal directions. For larger T_c , ΔH_{c2} becomes positive and the maxima of H_{c2} are shifted to nodal directions. Clearly, T_c has important impacts on the angular dependence of H_{c2} .

v_0 : We then consider the influence of fermion velocity v_0 , which characterizes the strength of the orbital effect. According to Fig. 5(b), H_{c2} is not a monotonic function of v_0 , it increases with v_0 for small values of v_0 but decreases with v_0 when v_0 is large enough. Therefore, in the presence of Pauli paramagnetic effect, the increasing of orbital effect does not necessarily suppress H_{c2} . At $v_0 = 0$, the orbital effect is removed, so the Pauli paramagnetic effect entirely determines H_{c2} . H_{c2} is then angle independent, and $\Delta H_{c2} = 0$. For finite v_0 , H_{c2} becomes angle dependent and exhibits fourfold oscillation, as a consequence of the interplay between orbital and Pauli paramagnetic effects. As shown in Fig. 6(b), ΔH_{c2} is negative for both small and large values of v_0 , but becomes positive for intermediate values of v_0 .

g : Taking $g = 0$ simply leads to the known results obtained in the case of pure orbital effect. From Fig 5(c), we see that H_{c2} monotonously decreases with the increase of g , which indicates the Pauli paramagnetic effect always tends to suppress H_{c2} . As depicted in Fig. 6(c), ΔH_{c2} is negative when g takes small values but positive when g becomes sufficiently large.

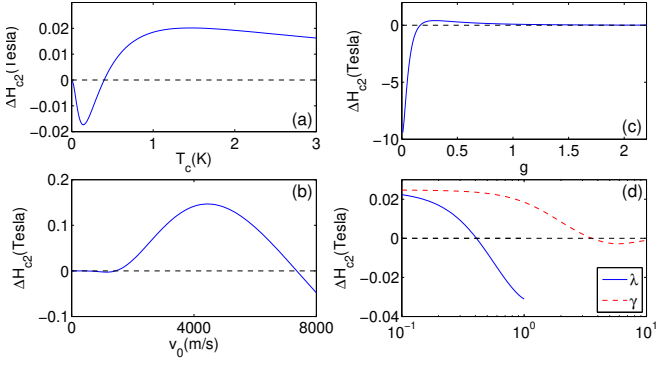


FIG. 6: (a) T_c -dependence of ΔH_{c2} . (b) v_0 -dependence of ΔH_{c2} . (c) g -dependence of ΔH_{c2} . (d) Blue solid line: λ -dependence of ΔH_{c2} . Red dashed line: γ -dependence of ΔH_{c2} . Parameters are the same as those of Fig. 5.

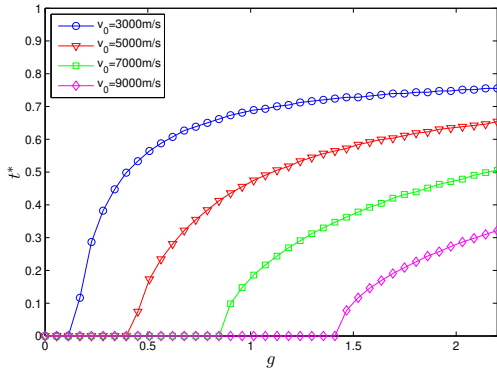


FIG. 7: Relation between g and t^* . $T_c = 1K$, $\lambda = 0.5$, $\gamma = 1$.

λ : For $t_c = \lambda = 0$, the rippled cylindrical Fermi surface reduces to a cylindrical Fermi surface. Figure 5(d) shows that H_{c2} decreases monotonously as λ increases. It appears that H_{c2} takes larger values as a three-dimensional superconductor evolves gradually to be quasi-two-dimensional. According to the blue solid line in Fig. 6(d), for given values of other parameters, the maxima of H_{c2} is along the nodal directions for small values of λ and antinodal directions for large values of λ .

γ : As shown in Fig 5(d), H_{c2} is a monotonic function of γ . Varying γ can also lead to similar $\pi/4$ shift in H_{c2} . According to the red dashed line in Fig. 6(d), for given relevant parameters, the maxima of H_{c2} is along nodal directions for small values of γ and antinodal directions for large values of γ .

From above results, we know that the detailed angular dependence of in-plane H_{c2} is significantly influenced by a number of physical parameters. The fourfold oscillation pattern of H_{c2} can be shifted by $\pi/4$ if we tune anyone of these parameters. The fact that H_{c2} may exhibit its maxima along either nodal or antinodal directions denies the naive expectation that H_{c2} always displays the same angular dependence as the d -wave gap. Therefore, one should be very careful when fitting theories with exper-

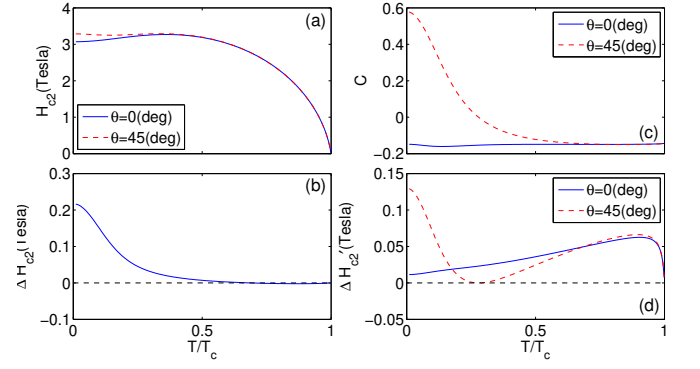


FIG. 8: (a), (b), (c) and (d): t -dependence of H_{c2} , ΔH_{c2} , C and $\Delta H'_{c2}$. $T_c = 1K$, $v_0 = 3000m/s$, $\lambda = 0.5$, $\gamma = 1$, and $g = 1$. Landau level mixing is included.

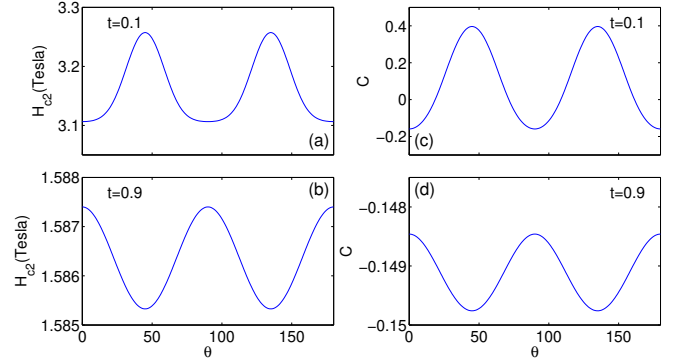


FIG. 9: Angular dependence of H_{c2} and C at $t = 0.1$ and $t = 0.9$. $T_c = 1K$, $v_0 = 3000m/s$, $\lambda = 0.5$, $\gamma = 1$, and $g = 1$. Landau level mixing is included

iments, because inaccurate and even wrong conclusions will be drawn if some of the parameters are not properly chosen. Due to the complicated dependence of H_{c2} on various parameters and inevitable approximations employed in the theoretical calculations, it is infeasible to identify the precise gap symmetry solely by measuring the fourfold oscillation of H_{c2} .

The temperature t plays a particular role since it is usually the only free parameter in one specific material. Our results show that there is generally a $\pi/4$ difference in the positions of the maxima of H_{c2} and those of d -wave gap for $t < t^* = T^*/T_c$, provided that g is sufficiently large. We emphasize that this conclusion does not depend on the specific values of other five parameters. Indeed, those five parameters change the fourfold oscillation of H_{c2} by altering the critical value T^* . However, H_{c2} and d -wave gap always exhibit their maxima at exactly the same angles once t exceeds t^* , which indicates that the Pauli paramagnetic effect is relatively weak compared to the orbital effect at higher T .

In order to better understand this point, we plot the relation between t^* and g for several values of velocity v_0 in Fig. 7. Since larger g represents stronger Pauli paramagnetic effect and larger v_0 describes stronger orbital

effect, this figure clearly shows how t^* is determined by the competition between the orbital and Pauli paramagnetic effects. The monotonic increase of t^* with growing g confirms the conclusion that strong Pauli paramagnetic effect causes the $\pi/4$ difference between the angular dependence of H_{c2} and d -wave gap.

IV. THE INFLUENCE OF LANDAU LEVEL MIXING AND FFLO STATE

In this section, we consider the influence of Landau level mixing and the FFLO state. In contrast to the isotropic s -wave superconductors, higher Landau level components of the order parameter are generally mixed in anisotropic superconductors, which was first emphasized by Luk'yanchuk and Mineev^{4,8-10,49,55}. In the case of d -wave pairing, symmetry arguments ensure that only the $N = 0$ and $N = 2$ Landau levels are allowed^{8-10,55}. FFLO state is a novel superconducting state induced by strong magnetic field where the corresponding Cooper pairing has a finite total momentum^{42,43,54,56,57}. In a FFLO state, the superconducting gap is modulated in the real space. There have appeared considerable experimental clues in the past decade suggesting that CeCoIn₅ is a possible candidate for the FFLO state^{20,37,57}.

Including the mixing between different Landau levels, the function $\Delta_\alpha(\mathbf{R})$ can be written as^{4,8-10}

$$\Delta_\alpha(\mathbf{R}) = [1 + C(a_+)^2] \Delta_0(\mathbf{R}), \quad (16)$$

where a_+ is the raising operator which is showed in Eq. (11), and C is the corresponding admixing parameter of the Landau levels. The corresponding equations for H_{c2} is found to have the form

$$-\ln(t) = \int_0^{+\infty} du \frac{1}{\sinh(u)} \left\{ 1 - \int_{-\pi}^{\pi} \frac{d\chi}{2\pi} \int_0^{2\pi} \frac{d\varphi}{2\pi} \times \cos(hu) [1 + \cos(4\varphi) \cos(4\theta)] \times \exp[-\rho u^2 S_1] [1 + 2C\rho u^2 S_2] \right\}, \quad (17)$$

and

$$-\ln(t)C = \int_0^{+\infty} du \frac{1}{\sinh(u)} \left\{ C - \int_{-\pi}^{\pi} \frac{d\chi}{2\pi} \int_0^{2\pi} \frac{d\varphi}{2\pi} \times \cos(hu) [1 + \cos(4\varphi) \cos(4\theta)] \times \exp[-\rho u^2 S_1] [\rho u^2 S_2 + C(1 - 4\rho u^2 S_1 + 2\rho^2 u^4 S_1^2)] \right\}, \quad (18)$$

where

$$S_1 = \lambda^2 \gamma^2 \sin^2 \chi + (1 + \lambda \cos \chi) \sin^2 \varphi, \quad (19)$$

$$S_2 = \lambda^2 \gamma^2 \sin^2 \chi - (1 + \lambda \cos \chi) \sin^2 \varphi. \quad (20)$$

We show the T -dependence of H_{c2} , C , ΔH_{c2} , and $\Delta' H_{c2}$ in Fig. 8, where $\Delta' H_{c2}$ represents the difference

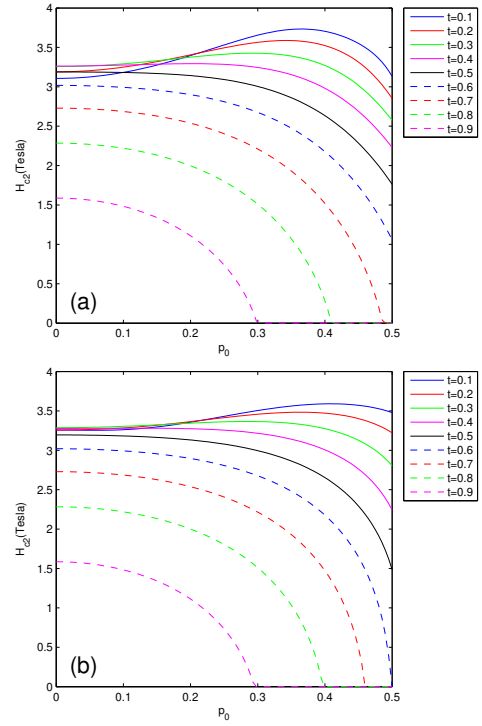


FIG. 10: The relation between H_{c2} and the parameter p_0 at different temperatures. The other parameters are chosen as $T_c = 1K$, $v_0 = 3000m/s$, $\lambda = 0.5$, $\gamma = 1$, and $g = 1$. (a) $\theta = 0^\circ$; (b) $\theta = 45^\circ$. Landau level mixing and influence of FFLO state are included.

of the values of H_{c2} with and without the Landau level mixing effects. The angular dependences of H_{c2} and C are plotted in Fig. 9. We find that including Landau level mixing does not change the general feature that the maximum of H_{c2} is along nodal directions at low T but along antinodal directions at higher T . Figure 8 also shows that $\Delta H'_{c2}$ is greater than zero, which simply means that the Landau level mixing enhances H_{c2} .

We now consider the impacts of both Landau level mixing and FFLO state. In this case, we should re-write $\Delta_\alpha(\mathbf{R})$ as⁹

$$\Delta_\alpha(\mathbf{R}) = \cos(\mathbf{q} \cdot \mathbf{R}) [1 + C(a_+)^2] \Delta_0(\mathbf{R}). \quad (21)$$

The equations for H_{c2} can be obtained by replacing the function $\cos(hu)$ appearing in Eqs. (17) and (18) with $\cos(hu) \cos[p u \cos(\varphi)]$, where $p = \frac{v_0 q}{2\pi T}$. A detailed derivation of the equations is presented in Appendix A.

The relations between H_{c2} and the FFLO parameter p_0 at different temperatures are shown in Fig. 10. Here, p_0 is given by $p_0 = \frac{v_0 q}{2\pi T}$, and p_{0r} denotes the physical value of p_0 that corresponds to the maximum value of H_{c2} . We find that p_{0r} takes a finite value at lower temperature, however, p_{0r} equals to zero when the temperature is larger than a critical value. After numerical calculation, we find the temperature dependence of H_{c2} , ΔH_{c2} , C and p_{0r} , as shown in Fig. 11. It is interesting that, once FFLO state is considered, the angular dependence

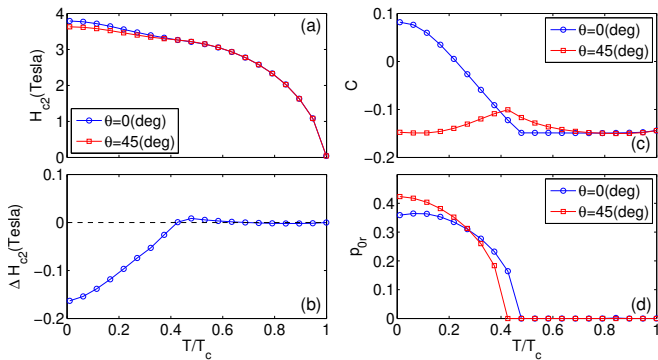


FIG. 11: Temperature dependence of H_{c2} , ΔH_{c2} , C and p_{0r} are shown in (a), (b), (c) and (d) respectively. The other parameters are chosen as $T_c = 1K$, $v_0 = 3000m/s$, $\lambda = 0.5$, $\gamma = 1$, and $g = 1$. Landau level mixing and influence of FFLO state are included.

of H_{c2} can be significantly modified. We can see that the maxima of H_{c2} is along the antinodal directions at low and high temperatures, but along the nodal directions at intermediate temperatures. Apparently, the existence of FFLO state makes it nearly impossible to probe the gap symmetry by measuring H_{c2} at some fixed temperature. Measuring the angular dependence of H_{c2} at a number of different temperatures is thus more reasonable.

V. COMPARISON WITH EXPERIMENTS

In this section, we compare our results with the experimental studies. There is a longstanding controversy on the in-plane H_{c2} of $CeCoIn_5$. Settai *et al.*³⁶ reported that the maxima of H_{c2} are along the [100] direction through de Haas-van Alphen oscillation experiments at 40mK. Bianchi *et al.*³⁷ found the maxima of H_{c2} along the [100] direction by measuring the specific heat at $T > 1K$. Weickert *et al.*⁹ measured the electric resistivity at 100mK and found the maxima of H_{c2} along the [100] direction. These measurements seem to agree with each other. However, Murphy *et al.*³⁵ observed the maxima of H_{c2} along the [110] direction in cantilever magnetometer measurements performed at 20mK. At first glance, the observation of Murphy *et al.*³⁵ is in sharp conflict with other measurements^{9,36,37}, and thus stands as an obstacle in the determination of the precise gap symmetry of $CeCoIn_5$.

Our theoretical analysis suggest that the above experimental results might be actually well consistent. Note that the measurements of Murphy *et al.*³⁵ are performed at 20mK, whereas all the others^{9,36,37} are performed at $T \geq 40mK$. The experimental discrepancy can be naturally resolved if, as predicted in our analysis, there is a $\pi/4$ shift in the angular dependence of H_{c2} at certain temperature between 20mK and 40mK. The critical point T^* at which H_{c2} shifts by $\pi/4$ can be probed by carefully measuring the angular dependence of in-plane H_{c2} at a

number of different temperatures falling in the range of $20mK < T < 40mK$.

It is also interesting to remark on the behavior of H_{c2} in $CeCu_2Si_2$. Different from a $d_{x^2-y^2}$ -wave gap symmetry deduced in most earlier investigations^{22,23}, a d_{xy} -wave symmetry was proposed by Vieyra *et al.*¹⁰ after comparing model calculations to the experimental data of H_{c2} measured at 40mK. This conclusion is problematic for two reasons. Firstly, as illustrated in our theoretic analysis, it is not appropriate to fit experimental results of angle-resolved H_{c2} at some fixed temperature. Secondly, in the equation of H_{c2} given in Ref.¹⁰, a rippled cylindrical Fermi surface is adopted. However, no tuning parameter is adopted in their calculations to characterize how rippled is the Fermi surface. Our analysis indicate that, in order to deduce an accurate gap symmetry from the experiments of in-plane H_{c2} , a more reasonable method is to measure the angular dependence of H_{c2} at a series of temperatures and to see whether there is a $\pi/4$ shift at certain critical temperature T^* .

VI. SUMMARY AND DISCUSSION

In summary, we have studied the angular dependence of in-plane upper critical field H_{c2} in some d -wave heavy fermion superconductors after including both the orbital and Pauli paramagnetic effects. By solving the equation of H_{c2} systematically, we have showed that whether H_{c2} exhibits its maxima along the nodal or antinodal direction crucially depends on a number of tuning parameters in the presence of a strong Pauli paramagnetic effect. This makes it difficult to entirely fix the d -wave gap symmetry, since a moderate variation of one or some of the tuning parameter can lead to a $\pi/4$ shift in the angular dependence of H_{c2} . Neglecting Landau level mixing and FFLO state, we have found a general property that H_{c2} always exhibits its maxima along the nodal directions at $T < T^*$ and the antinodal directions at $T^* < T < T_c$, where T^* is a critical temperature below T_c , provided that the Pauli paramagnetic effect is strong enough. When the Landau level mixing is included, this general property does not qualitatively change. However, the directions of maxima of H_{c2} take more complex dependence on temperature if the superconductor has a FFLO ground state.

Our theoretical studies have gone beyond previous works⁸⁻¹⁰ in several aspects. Firstly, in previous studies, a rippled cylindrical Fermi surface was employed, but there is not any effective parameter in the equations of H_{c2} to characterize the concrete shape of the Fermi surface. In our analysis, the shape of the rippled cylindrical Fermi surface is defined by two parameters, namely γ and λ . We have illustrated via careful calculations that tuning these two parameters can qualitatively alter the angular dependence of H_{c2} . Secondly, in previous studies, the angular dependence of H_{c2} was always calculated and then compared with experiments at cer-

tain given temperature. Our analysis have showed that whether the maxima of H_{c2} are along nodal or antinodal directions is determined by the values of a number of tuning parameters. Therefore, one should not identify the correct gap symmetry by measuring the angular dependence of H_{c2} at a fixed temperature. Instead, measuring the angular dependence of H_{c2} at a series of temperatures and examining whether there is a $\pi/4$ shift as the temperature varies is a better method. Thirdly, our studies provide a candidate solution to the long-standing experimental discrepancy about the angular dependence of H_{c2} in CeCoIn₅.

To gain a more convincing understanding of the angular dependence of in-plane H_{c2} and its application to realistic experiments of heavy fermion superconductors, our theoretic analysis may be improved in several aspects in the future. For instance, an important assumption used in our analysis is that the superconducting phase transition is second order, which has also been used broadly in previous works⁸⁻¹⁰. If the phase transition is first order, it would be difficult to derive an effective equation for H_{c2} .

In addition, we have employed in our work an ideal rippled cylindrical Fermi surface. It would be very interesting to generalize our consideration to superconductors with a more complicated and more realistic Fermi surface. We have also ignored the possible influence of multi-band effects, which was recently found to be important in several heavy fermion superconductors such as CeCu₂Si₂^{24-26,58} and CeCoIn₅^{33,34}. Finally, our analysis is essentially BCS mean-field treatment, which neglects correlation effects. The possible competition and coexistence between superconducting and antiferromagnetic orders may play some role^{53,59} and hence need to be incorporated in a more refined investigation of H_{c2} .

ACKNOWLEDGEMENTS

We acknowledge the support by the National Natural Science Foundation of China under Grants No.11504379, No.11274286, No.11574285, and No.U1532267.

Appendix A: Derivation of equation of H_{c2} in the presence of Landau level mixing and FFLO state

We will provide the detailed calculations of the equation of in-plane H_{c2} in the presence of both Landau level mixing and FFLO state. The linearized gap equation can be written as^{52,54}

$$\begin{aligned} -\ln\left(\frac{T}{T_c}\right)\Delta_\alpha(\mathbf{R}) &= \int_0^{+\infty} d\eta \frac{\pi T}{\sinh(\pi T\eta)} \int_{-\pi}^{\pi} \frac{d\chi}{2\pi} \int_0^{2\pi} \frac{d\varphi}{2\pi} \left[\gamma_\alpha(\hat{\mathbf{k}})\right]^2 \left[\frac{1}{2} - \frac{\exp(ih\eta)}{2} \exp(L_1)\right] \Delta_\alpha(\mathbf{R}) \\ &+ \int_0^{+\infty} d\eta \frac{\pi T}{\sinh(\pi T\eta)} \int_{-\pi}^{\pi} \frac{d\chi}{2\pi} \int_0^{2\pi} \frac{d\varphi}{2\pi} \left[\gamma_\alpha(\hat{\mathbf{k}})\right]^2 \left[\frac{1}{2} - \frac{\exp(-ih\eta)}{2} \exp(-L_1)\right] \Delta_\alpha(\mathbf{R}), \end{aligned} \quad (\text{A1})$$

where

$$L_1 = \frac{1}{2}i\eta\sqrt{eH} \left[(v_a \sin(\theta - \varphi) + iv_c \sin(\chi)) a_+ + (v_a \sin(\theta - \varphi) - iv_c \sin(\chi)) a_- + \sqrt{2}v_a \cos(\theta - \varphi) a_0 \right]. \quad (\text{A2})$$

We assume that $\Delta_\alpha(\mathbf{R})$ takes the FFLO state⁹

$$\Delta_\alpha(\mathbf{R}) = \cos(\mathbf{q} \cdot \mathbf{R}) \left[1 + C(a_+)^2 \right] \Delta_0(\mathbf{R}) \quad (\text{A3})$$

with

$$\Delta_0(\mathbf{R}) = \left(\sqrt{\frac{2eH}{\pi}} \right)^{\frac{1}{2}} \exp \left[-eH (x \sin \theta - y \cos \theta)^2 \right]. \quad (\text{A4})$$

Here, \mathbf{q} is along the direction of the magnetic field, namely $\mathbf{q} = q[\cos \theta \mathbf{e}_x + \sin \theta \mathbf{e}_y]$. Therefore it is easy to get $\cos(\mathbf{q} \cdot \mathbf{R}) = \cos[q(x \cos \theta + y \sin \theta)]$. One can verify that

$$a_- \Delta_0 = 0, \quad [a_\pm, \cos(\mathbf{q} \cdot \mathbf{R})] = 0, \quad [a_0, \cos(\mathbf{q} \cdot \mathbf{R})] = \sum_{\sigma=\pm 1} \frac{\sigma q}{(2eH)^{\frac{1}{2}}} \frac{\exp[i\sigma q(x \cos \theta + y \sin \theta)]}{2}. \quad (\text{A5})$$

Substituting Eq. (A3) into Eq. (A1), we obtain

$$-\ln\left(\frac{T}{T_c}\right) \cos(\mathbf{q} \cdot \mathbf{R}) \left[1 + C(a_+)^2 \right] \Delta_0(\mathbf{R})$$

$$\begin{aligned}
&= \int_0^{+\infty} d\eta \frac{\pi T}{\sinh(\pi T \eta)} \int_{-\pi}^{\pi} \frac{d\chi}{2\pi} \int_0^{2\pi} \frac{d\varphi}{2\pi} [\gamma_\alpha(\hat{\mathbf{k}})]^2 \left[\frac{1}{2} - \frac{\exp(ih\eta)}{2} \exp(L_1) \right] \cos(\mathbf{q} \cdot \mathbf{R}) [1 + C(a_+)^2] \Delta_0(\mathbf{R}) \\
&\quad + \int_0^{+\infty} dt \frac{\pi T}{\sinh(\pi T \eta)} \int_{-\pi}^{\pi} \frac{d\chi}{2\pi} \int_0^{2\pi} \frac{d\varphi}{2\pi} [\gamma_\alpha(\hat{\mathbf{k}})]^2 \left[\frac{1}{2} - \frac{\exp(-ih\eta)}{2} \exp(-L_1) \right] \cos(\mathbf{q} \cdot \mathbf{R}) [1 + C(a_+)^2] \\
&\quad \times \Delta_0(\mathbf{R}).
\end{aligned} \tag{A6}$$

Exchanging the position of $1 + C(a_+)^2$ and $\cos(\mathbf{q} \cdot \mathbf{R})$ leads us to

$$\begin{aligned}
& - \ln\left(\frac{T}{T_c}\right) [1 + C(a_+)^2] \cos(\mathbf{q} \cdot \mathbf{R}) \Delta_0(\mathbf{R}) \\
&= \int_0^{+\infty} d\eta \frac{\pi T}{\sinh(\pi T \eta)} \int_{-\pi}^{\pi} \frac{d\chi}{2\pi} \int_0^{2\pi} \frac{d\varphi}{2\pi} [\gamma_\alpha(\hat{\mathbf{k}})]^2 \left\{ \frac{1}{2} [1 + C(a_+)^2] \cos(\mathbf{q} \cdot \mathbf{R}) - \frac{\exp(ih\eta)}{2} \right. \\
&\quad \times L_3(\eta) \exp(L_2) L_4(\eta) \} \Delta_0(\mathbf{R}) \\
&\quad + \int_0^{+\infty} d\eta \frac{\pi T}{\sinh(\pi T \eta)} \int_{-\pi}^{\pi} \frac{d\chi}{2\pi} \int_0^{2\pi} \frac{d\varphi}{2\pi} [\gamma_\alpha(\hat{\mathbf{k}})]^2 \left\{ \frac{1}{2} [1 + C(a_+)^2] \cos(\mathbf{q} \cdot \mathbf{R}) - \frac{\exp(-ih\eta)}{2} \right. \\
&\quad \times L_3(-\eta) \exp(-L_2) L_4(-\eta) \} \Delta_0(\mathbf{R}),
\end{aligned} \tag{A7}$$

where

$$L_2(\eta) = \frac{i}{2} \eta \sqrt{eH} [(v_a \sin(\theta - \varphi) + iv_c \sin(\chi)) a_+ + (v_a \sin(\theta - \varphi) - iv_c \sin(\chi)) a_-], \tag{A8}$$

$$L_3(\eta) = 1 + C \left[(a_+)^2 + i\eta(eH)^{\frac{1}{2}} (v_a \sin(\theta - \varphi) - iv_c \sin(\chi)) a_+ + \left(\frac{i}{2} \eta(eH)^{\frac{1}{2}} (v_a \sin(\theta - \varphi) - iv_c \sin(\chi)) \right)^2 \right] \tag{A9}$$

$$L_4(\eta) = \sum_{\sigma=\pm 1} \exp \left[\frac{i}{2} \eta \sigma v_a q \cos(\theta - \varphi) \right] \frac{\exp(i\sigma \mathbf{q} \cdot \mathbf{R})}{2}. \tag{A10}$$

In the above derivation, we have used the formula

$$[\hat{A}, e^{\hat{B}}] = \hat{C} e^{\hat{B}}, \tag{A11}$$

where \hat{A} and \hat{B} do not commute with each other. If $\hat{C} = [\hat{A}, \hat{B}]$, then \hat{C} commutes with \hat{A} and \hat{B} , namely $[\hat{A}, \hat{C}] = 0$ and $[\hat{B}, \hat{C}] = 0$. Multiplying $(a_-)^2$ on both sides of the Eq. (A6), and then moving a_+ leftwards and a_- rightwards, we find that

$$\begin{aligned}
& - \ln\left(\frac{T}{T_c}\right) 2C \cos(\mathbf{q} \cdot \mathbf{R}) \Delta_0(\mathbf{R}) \\
&= \int_0^{+\infty} d\eta \frac{\pi T}{\sinh(\pi T \eta)} \int_{-\pi}^{\pi} \frac{d\chi}{2\pi} \int_0^{2\pi} \frac{d\varphi}{2\pi} [\gamma_\alpha(\hat{\mathbf{k}})]^2 \left[C \cos(\mathbf{q} \cdot \mathbf{R}) - \frac{\exp(ih\eta)}{2} L_5(\eta) \exp(L_2) L_4(\eta) \right] \Delta_0(\mathbf{R}) \\
&\quad + \int_0^{+\infty} d\eta \frac{\pi T}{\sinh(\pi T \eta)} \int_{-\pi}^{\pi} \frac{d\chi}{2\pi} \int_0^{2\pi} \frac{d\varphi}{2\pi} [\gamma_\alpha(\hat{\mathbf{k}})]^2 \left[C \cos(\mathbf{q} \cdot \mathbf{R}) - \frac{\exp(-ih\eta)}{2} L_5(-\eta) \exp(-L_2) L_4(-\eta) \right] \Delta_0(\mathbf{R}),
\end{aligned} \tag{A12}$$

where

$$\begin{aligned}
L_5(\eta) &= 2C + 2C \left[2a_+ + i\eta(eH)^{1/2} (v_a \sin(\theta - \varphi) - iv_c \sin(\chi)) \right] \left(\frac{i}{2} \eta(eH)^{1/2} (v_a \sin(\theta - \varphi) + iv_c \sin(\chi)) \right) \\
&\quad + \left[1 + C(a_+)^2 + C i\eta(eH)^{1/2} (v_a \sin(\theta - \varphi) - iv_c \sin(\chi)) a_+ \right. \\
&\quad \left. + C \left(\frac{i}{2} \eta(eH)^{1/2} (v_a \sin(\theta - \varphi) - iv_c \sin(\chi)) \right)^2 \right] \left(\frac{i}{2} \eta(eH)^{1/2} (v_a \sin(\theta - \varphi) + iv_c \sin(\chi)) \right)^2.
\end{aligned} \tag{A13}$$

It is necessary to make an average of Eqs. (A7) and (A12) on the ground state $\Delta_0(\mathbf{R})$. Since $\Delta_0(\mathbf{R})$ takes the form of the eigenfunction of harmonic oscillators, we can use the formula for harmonic oscillators:

$$\langle e^{\hat{A}} \rangle = e^{\frac{1}{2} \langle \hat{A}^2 \rangle}, \tag{A14}$$

and then obtain

$$-\ln\left(\frac{T}{T_c}\right) = \int_0^{+\infty} d\eta \frac{\pi T}{\sinh(\pi T \eta)} \left\{ 1 - \cos(h\eta) \cos\left[\frac{1}{2}\eta v_a q \cos(\theta - \varphi)\right] \int_{-\pi}^{\pi} \frac{d\chi}{2\pi} \int_0^{2\pi} \frac{d\varphi}{2\pi} [\gamma_\alpha(\hat{\mathbf{k}})]^2 \right. \\ \left. \times \exp\left[-\frac{\eta^2 e H}{8} [v_a^2 \sin^2(\theta - \varphi) + v_c^2 \sin^2(\chi)]\right] \left[1 + \frac{C}{4} \eta^2 e H (v_c^2 \sin^2(\chi) - v_a^2 \sin^2(\theta - \varphi))\right] \right\} \quad (\text{A15})$$

and

$$-\ln\left(\frac{T}{T_c}\right) 2C = \int_0^{+\infty} d\eta \frac{\pi T}{\sinh(\pi T \eta)} \left\{ 2C - \cos(h\eta) \cos\left[\frac{1}{2}\eta v_a q \cos(\theta - \varphi)\right] \int_{-\pi}^{\pi} \frac{d\chi}{2\pi} \int_0^{2\pi} \frac{d\varphi}{2\pi} [\gamma_\alpha(\hat{\mathbf{k}})]^2 \right. \\ \times \exp\left[-\frac{\eta^2 e H}{8} [v_a^2 \sin^2(\theta - \varphi) + v_c^2 \sin^2(\chi)]\right] \left[\frac{1}{4} \eta^2 e H (v_c^2 \sin^2(\chi) - v_a^2 \sin^2(\theta - \varphi)) \right. \\ \left. + 2C \left(1 - \frac{1}{2} \eta^2 e H (v_a^2 \sin^2(\theta - \varphi) + v_c^2 \sin^2(\chi)) + \frac{1}{32} \eta^4 e^2 H^2 (v_a^2 \sin^2(\theta - \varphi) + v_c^2 \sin^2(\chi))^2\right) \right] \left. \right\}. \quad (\text{A16})$$

Substituting $[\gamma_\alpha(\hat{\mathbf{k}})]^2 = 1 + \cos(4\varphi)$ into Eqs. (A15) and (A16) and defining $\pi T \eta = u$, we eventually find that

$$-\ln(t) = \int_0^{+\infty} du \frac{1}{\sinh(u)} \left\{ 1 - \cos(hu) \cos[pu \cos(\varphi)] \int_{-\pi}^{\pi} \frac{d\chi}{2\pi} \int_0^{2\pi} \frac{d\varphi}{2\pi} [1 + \cos(4\varphi) \cos(4\theta)] \right. \\ \times \exp\left[-\rho u^2 \left(\left(\frac{v_c}{v_a}\right)^2 \sin^2(\chi) + \sin^2(\varphi)\right)\right] \left[1 + 2C \rho u^2 \left(\left(\frac{v_c}{v_a}\right)^2 \sin^2(\chi) - \sin^2(\varphi)\right)\right] \left. \right\} \quad (\text{A17})$$

and

$$-\ln(t)C = \int_0^{+\infty} du \frac{1}{\sinh(u)} \left\{ C - \cos(hu) \cos[pu \cos(\varphi)] \int_{-\pi}^{\pi} \frac{d\chi}{2\pi} \int_0^{2\pi} \frac{d\varphi}{2\pi} [1 + \cos(4\varphi) \cos(4\theta)] \right. \\ \times \exp\left[-\rho u^2 \left(\left(\frac{v_c}{v_a}\right)^2 \sin^2(\chi) + \sin^2(\varphi)\right)\right] \left[\rho u^2 \left(\left(\frac{v_c}{v_a}\right)^2 \sin^2(\chi) - \sin^2(\varphi)\right) \right. \\ \left. + C \left(1 - 4\rho u^2 \left(\left(\frac{v_c}{v_a}\right)^2 \sin^2(\chi) + \sin^2(\varphi)\right) + 2\rho^2 u^4 \left(\left(\frac{v_c}{v_a}\right)^2 \sin^2(\chi) + \sin^2(\varphi)\right)^2\right) \right] \left. \right\}, \quad (\text{A18})$$

where

$$t = \frac{T}{T_c}, \quad h = \frac{g\mu_B H}{2\pi T}, \quad \rho = \frac{eHv_a^2}{8\pi^2 T^2}, \quad p = \frac{v_a q}{2\pi T}. \quad (\text{A19})$$

* wangjr@mail.ustc.edu.cn

† gzliu@ustc.edu.cn

¹ M. R. Norman, Science **332**, 196 (2011).

² D. J. Scalapino, Rev. Mod. Phys. **84**, 1383 (2012).

³ L. P. Gorkov, Pis'ma Zh. Eksp. Theor. Fiz. **40**, 351 (1984) [Sov. Phys. JETP Letter **40**, 1155 (1984)].

⁴ H. Won and K. Maki, Physica B **199-200**, 353 (1994).

⁵ K. Takanaka and K. Kuboya, Phys. Rev. Lett. **75**, 323 (1995).

⁶ Y. Koike, T. Takabayashi, T. Noji, T. Nishizaki, and N. Kobayashi, Phys. Rev. B **54**, R776 (1996).

⁷ T. Naito, S. Haraguchi, H. Iwasaki, T. Sasaki, T. Nishizaki, K. Shibata, and N. Kobayashi, Phys. Rev. B **63**, 172506 (2001).

⁸ H. Won, K. Maki, S. Haas, N. Oeschler, F. Weickert, P. Gegenwart, Phys. Rev. B **69**, 180504(R) (2004).

⁹ F. Weickert, P. Gegenwart, H. Won, D. Parker, and K. Maki, Phys. Rev. B **74**, 134511 (2006).

¹⁰ H. A. Vieyra, N. Oeschler, S. Seiro, H. S. Jeevan, C. Geibel, D. Parker, and F. Steglich, Phys. Rev. Lett. **106**, 207001 (2011).

¹¹ J. Murphy, M. A. Tanatar, D. Graf, J. S. Brooks, S. L.

- Bud'ko, P. C. Canfield, V. G. Kogan, and R. Prozorov, *Phys. Rev. B* **87**, 094505 (2013).
- ¹² Z. Q. Mao, Y. Maeno, S. Nishizaki, T. Akima, and T. Ishiguro, *Phys. Rev. Lett.* **84**, 991 (2000).
 - ¹³ H. Zuo, J.-K. Bao, Y. Liu, J. Wang, Z. Jin, Z. Xia, L. Li, Z. Xu, Z. Zhu, and G.-H. Cao, arXiv:1511.06169v1.
 - ¹⁴ C. C. Tsuei and J. R. Kirtley, *Rev. Mod. Phys.* **72**, 969 (2000).
 - ¹⁵ A. Damascelli, Z. Hussain, and Z.-X. Shen, *Rev. Mod. Phys.* **75**, 473 (2003).
 - ¹⁶ H. v. Löhneysen, A. Rosch, M. Vojta, and P. Wölfle, *Rev. Mod. Phys.* **79**, 1015 (2007).
 - ¹⁷ O. Stockert, S. Kirchner, F. Steglich, and Q. Si, *J. Phys. Soc. Jpn.* **81**, 011001 (2012).
 - ¹⁸ Y. Matsuda, K. Izawa and I. Vekhter, *J. Phys.: Condens. Matter* **18**, R705 (2006).
 - ¹⁹ J. L. Sarrao and J. D. Thompson, *J. Phys. Soc. Jpn.* **76**, 051013 (2007).
 - ²⁰ J. D. Thompson and Z. Fisk, *J. Phys. Soc. Jpn.* **81**, 011002 (2012).
 - ²¹ F. Steglich, J. Aarts, C. D. Bredl, W. Lieke, D. Meschede, W. Franz, and H. Schäfer, *Phys. Rev. Lett.* **43**, 1892 (1979).
 - ²² O. Stockert, J. Arndt, A. Schneidewind, H. Schneider, H. S. Jeevan, C. Geibel, F. Steglich, M. Loewenhaupt, *Physica B* **403**, 973 (2008).
 - ²³ I. Eremin, G. Zwirgmaier, P. Thalmeier, and P. Fulde, *Phys. Rev. Lett.* **101**, 187001 (2008).
 - ²⁴ S. Kittaka, Y. Aoki, Y. Shimura, T. Sakakibara, S. Seiro, C. Geibel, F. Steglich, H. Ikeda, and K. Machida, *Phys. Rev. Lett.* **112**, 067002 (2014).
 - ²⁵ M. Enayat, Z. Sun, A. Maldonado, H. Suderow, S. Seiro, C. Geibel, S. Wirth, F. Steglich, and P. Wahl, *Phys. Rev. B* **93**, 045123 (2016).
 - ²⁶ H. Ikeda, M.-T. Suzuki, and R. Arita, *Phys. Rev. Lett.* **114**, 147003 (2015).
 - ²⁷ G. M. Pang, M. Smidman, J. L. Zhang, L. Jiao, Z. F. Weng, E. M. Nica, Y. Chen, W. B. Jiang, Y. J. Zhang, H. S. Jeevan, P. Gegenwart, F. Steglich, Q. Si, and H. Q. Yuan, arXiv:1605.04786v1.
 - ²⁸ C. Petrovic, P. G. Pagliuso, M. F. Hundley, R. Movshovich, J. L. Sarrao, J. D. Thompson, Z. Fisk, and P. Monthoux, *J. Phys.: Condens. Matter* **13**, L337 (2001).
 - ²⁹ K. Izawa, H. Yamaguchi, Y. Matsuda, H. Shishido, R. Settai, and Y. Onuki, *Phys. Rev. Lett.* **87**, 057002 (2001).
 - ³⁰ K. An, T. Sakakibara, R. Settai, Y. Onuki, M. Hiragi, M. Ichioka, and K. Machida, *Phys. Rev. Lett.* **104**, 037002 (2010).
 - ³¹ W. K. Park, J. L. Sarrao, J. D. Thompson, and L. H. Greene, *Phys. Rev. Lett.* **100**, 177001 (2008).
 - ³² C. Stock, C. Broholm, J. Hudis, H. J. Kang, and C. Petrovic, *Phys. Rev. Lett.* **100**, 087001 (2008).
 - ³³ M. P. Allan, F. Massee, D. K. Morr, J. Van Dyke, A. W. Rost, A. P. Mackenzie, C. Petrovic, and J. C. Davis, *Nat. Phys.* **9**, 468(2013).
 - ³⁴ B. B. Zhou, S. Misra, E. H. da Silva Neto, P. Aynajian, R. E. Baumbach, J. D. Thompson, E. D. Bauer, and A. Yazdani, *Nat. Phys.* **9**, 474 (2013).
 - ³⁵ T. P. Murphy, D. Hall, E. C. Palm, S. W. Tozer, C. Petrovic, Z. Fisk, R. G. Goodrich, P. G. Pagliuso, J. L. Sarrao, and J. D. Thompson, *Phys. Rev. B* **65**, 100514(R) (2002).
 - ³⁶ R. Settai, H. Shishido, S. Ikeda, Y. Murakawa, M. Nakashima, D. Aoki, Y. Haga, H. Harima, and Y. Ōnuki, *J. Phys.: Condens Matter* **13**, L627 (2001).
 - ³⁷ A. Bianchi, R. Movshovich, C. Capan, P. G. Pagliuso, and J. L. Sarrao, *Phys. Rev. Lett.* **91**, 187004 (2003).
 - ³⁸ T. Das, A. B. Vorontsov, I. Vekhter, and M. J. Graf, *Phys. Rev. B* **87**, 174514 (2013).
 - ³⁹ A. Bianchi, R. Movshovich, N. Oeschler, P. Gegenwart, F. Steglich, J. D. Thompson, P. G. Pagliuso, and J. L. Sarrao, *Phys. Rev. Lett.* **89**, 137002 (2002).
 - ⁴⁰ A. D. Bianchi, M. Kenzelmann, L. DeBeer-Schmitt, J. S. White, E. M. Forgan, J. Mesot, M. Zolliker, J. Kohlbrecher, R. Movshovich, E. D. Bauer, J. L. Sarrao, Z. Fisk, C. Petrović, M. R. Eskildsen, *Science* **319**, 177 (2008).
 - ⁴¹ A. B. Vorontsov and I. Vekhter, *Phys. Rev. B* **81**, 094527 (2010).
 - ⁴² P. Fulde and R. A. Ferrell, *Phys. Rev. Lett.* **135**, A550 (1964).
 - ⁴³ A. I. Larkin and Y. N. Ovchinnikov, *Zh. Eksp. Teor. Phys.* **47**, 1136 (1964) [*Sov. Phys. JETP* **20**, 762 (1965)].
 - ⁴⁴ A. V. Chubukov and L. P. Gor'kov, *Phys. Rev. Lett.* **101**, 147004 (2008).
 - ⁴⁵ A. B. Vorontsov and I. Vekhter, *Phys. Rev. B* **75**, 224501 (2007).
 - ⁴⁶ P. Thalmeier, T. Watanabe, K. Izawa, Y. Matsuda, *Phys. Rev. B* **72**, 024539 (2005).
 - ⁴⁷ E. Helfand and N. R. Werthamer, *Phys. Rev.* **147**, 288 (1966).
 - ⁴⁸ N. R. Werthamer, E. Helfand, P. C. Hohenberg, *Phys. Rev.* **147**, 295 (1966).
 - ⁴⁹ I. A. Luk'yanchuk and V. P. Mineev, *Zh. Eksp. Teor. Phys.* **93**, 2045 (1987) [*Sov. Phys. JETP* **66**, 1168 (1987)].
 - ⁵⁰ K. Scharnberg and R. A. Klemm, *Phys. Rev. B* **22**, 5233 (1980).
 - ⁵¹ H. Shimahara, S. Matsuo, and K. Nagai, *Phys. Rev. B* **53**, 12284 (1996).
 - ⁵² H. Shimahara and D. Rainer, *J. Phys. Soc. Jpn.* **66**, 3591 (1997).
 - ⁵³ Y. Suginishi and H. Shimahara, *Phys. Rev. B* **74**, 024518 (2006).
 - ⁵⁴ H. Shimahara, *Phys. Rev. B* **80**, 214512 (2009).
 - ⁵⁵ H. Won and K. Maki, *Phys. Rev. B* **53**, 5927 (1996).
 - ⁵⁶ R. Casalbuoni and G. Nardulli, *Rev. Mod. Phys.* **76**, 263 (2004).
 - ⁵⁷ Y. Matsuda and H. Shimahara, *J. Phys. Soc. Jpn.* **76**, 051005 (2007).
 - ⁵⁸ Y. Tsutsumi, K. Machida, and M. Ichioka, *Phys. Rev. B* **92**, 020502(R) (2015).
 - ⁵⁹ G. Zwirgmaier and P. Fulde, *Z. Phys. B* **43**, 23 (1981).